



Synthesis, characterisation and magnetic properties of cobalt (II) complexes with 3-hydroxypicolinic acid (HpicOH): [Co(picOH)₂(H₂O)₂] and *mer*-[N(CH₃)₄][Co(picOH)₃] · H₂O

Penka I. Girginova^a, Filipe A. Almeida Paz^{a,b}, Helena I.S. Nogueira^a, Nuno J.O. Silva^c,
Vítor S. Amaral^c, Jacek Klinowski^b, Tito Trindade^{a,*}

^a Department of Chemistry, CICECO, University of Aveiro, Campus Santiago, 3810-193 Aveiro, Portugal

^b Department of Chemistry, University of Cambridge, Lensfield Road, CB2 1EW Cambridge, UK

^c Department of Physics, CICECO, University of Aveiro, 3810-193 Aveiro, Portugal

Received 10 December 2004; accepted 24 January 2005

Abstract

Two complexes with Co²⁺ and 3-hydroxypicolinic acid, [Co(picOH)₂(H₂O)₂] (**I**) and *mer*-[N(CH₃)₄][Co(picOH)₃] · H₂O (**II**), have been synthesised and characterised using single-crystal X-ray diffraction, elemental analysis, infrared spectroscopy, and thermoanalytical measurements. The 3-hydroxypicolinate ligands are coordinated to the Co²⁺ centres via its typical N,O-chelating coordination fashion. While in **I** the presence of two coordinated water molecules leads to the formation of a neutral [Co(picOH)₂(H₂O)₂] complex which is strongly hydrogen bonded to another four neighbouring complexes, in **II** the inclusion of a third picOH[−] ligand leads to an anionic octahedral complex, [Co(picOH)₃][−], in which all the N- and O-atoms are occupying *mer* positions. The properties of these two compounds were further investigated by measuring their magnetic behaviour.

© 2005 Elsevier Ltd. All rights reserved.

Keywords: Cobalt complexes; Crystal structures; 3-Hydroxypicolinic acid; Magnetic properties

1. Introduction

3-Hydroxypicolinic acid (HpicOH) is a relatively simple organic molecule, which can act as a versatile ligand with distinct coordination fashions. For example, deprotonation of the carboxylic acid and hydroxyl groups makes O,O-chelation possible with the consequent formation of a typical six-membered chelate ring [1–3]. The mono-deprotonated ligand (picOH[−]) can also form five-membered chelate rings through the pyridinic nitrogen atom and the carboxylate group (N,O-chelation) with this coordination fashion being the most commonly found in the literature [1–9]. Interestingly, there is only

one report for single coordination through the pyridinic nitrogen atom [6], and no examples are known of single coordination via the (de)protonated hydroxyl group.

We have exploited the versatile chelating properties of HpicOH to synthesise a series of lanthanide complexes and investigate the role of this ligand in the photoluminescence of the materials [1]. However, HpicOH is more commonly used with second- and third-row transition metal centres [5–8], and only a handful of structures containing first-row transition cations are found in the literature [2–4,9]. Other derivatives of picolinic acid are also known to form complexes with several metal centres [10,11], particularly those of 2-hydroxynicotinic acid which are of special interest [12,13]. Following our interest in exploring the coordination chemistry of HpicOH, we report on the synthesis, structural characterisation and magnetic behaviour of two novel Co²⁺

* Corresponding author. Tel.: +351 234 370 726; fax: +351 234 370 084.

E-mail address: ttrindade@dq.ua.pt (T. Trindade).

complexes with this ligand: $[\text{Co}(\text{picOH})_2(\text{H}_2\text{O})_2]$ and $\text{mer-}[\text{N}(\text{CH}_3)_4][\text{Co}(\text{picOH})_3] \cdot \text{H}_2\text{O}$.

2. Experimental

2.1. Syntheses

Chemicals were readily available from commercial sources and were used as received without further purification. Syntheses were carried out in PTFE-lined stainless steel reaction vessels (ca. 40 cm³), under autogeneous pressure and static conditions in a preheated oven at 150 °C. Reactions took place over a period of 48 h after which time the vessels were cooled slowly to ambient temperature before opening.

In a typical synthesis, an aqueous solution of $\text{CoCl}_2 \cdot 6\text{H}_2\text{O}$ (0.5 mmol) was added dropwise to an aqueous solution containing 3-hydroxypicolinic acid (2 mmol) and $[(\text{CH}_3)_4\text{N}]\text{OH}$ (2 mmol) and then the final pH was adjusted to ca. 7 with 1 M CH_3COOH . This mixture was treated under hydrothermal conditions as described above and then transferred into a covered beaker. A pale orange powder of $[\text{Co}(\text{picOH})_2(\text{H}_2\text{O})_2]$ was obtained (yield: 15.7%) and orange single-crystals of the same compound were grown after 10 days from the supernatant solution (m.p. 160 °C). Red crystals of $\text{mer-}[\text{N}(\text{CH}_3)_4][\text{Co}(\text{picOH})_3] \cdot \text{H}_2\text{O}$ could be obtained from the same mother solution after ca. 2 months (m.p. 228 °C).

2.2. Single-crystal X-ray diffraction

Suitable single-crystals of $[\text{Co}(\text{picOH})_2(\text{H}_2\text{O})_2]$ (**I**) and $\text{mer-}[\text{N}(\text{CH}_3)_4][\text{Co}(\text{picOH})_3] \cdot \text{H}_2\text{O}$ (**II**) were mounted on a glass fibre using perfluoropolyether oil [14]. Data for **I** were collected at 180(2) K on a Nonius Kappa charge coupled device (CCD) area-detector diffractometer (Mo $\text{K}\alpha$ graphite-monochromated radiation, $\lambda = 0.7107 \text{ \AA}$), equipped with an Oxford Cryosystems cryostream and controlled by the COLLECT software package [15]. Images were processed using the software packages of Denzo and Scalepack [16] and the data were corrected for absorption by using the empirical method employed in Sortav [17,18]. Data for **II** were collected at ambient temperature (at the Unidade de Raios-X, RIAIDT, University of Santiago de Compostela, Spain) on a Bruker SMART 1000 charge coupled device (CCD) area-detector diffractometer (Mo $\text{K}\alpha$ graphite-monochromated radiation, $\lambda = 0.7107 \text{ \AA}$), controlled by the SMART software package [19]. Images were processed using the SAINTPlus software package [20] and data were corrected for absorption by using the semi-empirical method of SADABS [21]. The two structures were solved by the direct methods of SHELXS-97 [22] and refined by full-matrix least squares

on F^2 using SHELXL-97 [23]. Non-hydrogen atoms were directly located from difference Fourier maps and refined with anisotropic displacement parameters. The last difference Fourier map synthesis showed, for **I**, the highest peak (0.354 e \AA^{-3}) located at 1.14 Å from O(2), and the deepest hole ($-0.614 \text{ e \AA}^{-3}$) located at 0.70 Å from Co(1); for **II**, the highest peak (0.389 e \AA^{-3}) located at 0.84 Å from O(4), and the deepest hole ($-0.490 \text{ e \AA}^{-3}$) located at 0.67 Å from Co(1).

Hydrogen atoms bound to carbon were placed in calculated positions and refined using a riding model with an isotropic displacement parameter fixed at x times U_{eq} for the atom to which they are attached ($x = 1.5$ for $-\text{CH}_3$ and $-\text{OH}$ groups, $x = 1.2$ for the remaining hydrogen atoms). Hydrogen atoms from water molecules were directly located from successive difference Fourier maps and refined with the O–H and H···H distances restrained to 0.95(1) and 1.55(1) Å (for **I**), and 0.85(1) and 1.39(1) Å (for **II**), respectively (in order to ensure a chemically reasonable geometry for these molecules), and using a riding model with an isotropic displacement parameter fixed at 1.5 times U_{eq} of the atom to which they are attached. Hydrogen atoms associated with the $-\text{OH}$ groups could also be directly located in successive difference Fourier maps, but their position was instead placed geometrically using HFIX instructions in SHELXL.

Table 1
Crystal and structure refinement data for $[\text{Co}(\text{picOH})_2(\text{H}_2\text{O})_2]$ (**I**) and $\text{mer-}[\text{N}(\text{CH}_3)_4][\text{Co}(\text{picOH})_3] \cdot \text{H}_2\text{O}$ (**II**)

	I	II
Formula	$\text{C}_{12}\text{H}_{12}\text{CoN}_2\text{O}_8$	$\text{C}_{22}\text{H}_{24}\text{CoN}_4\text{O}_9 \cdot \text{H}_2\text{O}$
Formula weight	371.17	565.40
Temperature (K)	180(2)	180(2)
Crystal system	monoclinic	monoclinic
Space group	$P2_1/c$	$P2_1/n$
a (Å)	11.491(2)	8.2794(20)
b (Å)	9.1413(18)	12.8360(32)
c (Å)	6.8357(14)	23.5421(57)
β (°)	91.84(3)	97.021(4)
Volume (Å ³)	717.7(2)	2483.2(11)
Z	2	4
D_c (g cm ⁻³)	1.718	1.512
μ (Mo $\text{K}\alpha$) (mm ⁻¹)	1.241	0.754
$F(000)$	378	1172
Crystal size (mm)	0.35 × 0.23 × 0.18	0.36 × 0.20 × 0.15
Crystal type	brown blocks	orange prisms
θ Range	3.55–27.49	3.57–26.42
Index ranges	$-14 \leq h \leq 14$, $-11 \leq k \leq 11$, $-8 \leq l \leq 8$	$-10 \leq h \leq 10$, $0 \leq k \leq 16$, $0 \leq l \leq 29$
Reflections collected	5621	21 304
Independent reflections	1638 ($R_{\text{int}} = 0.0407$)	5075 ($R_{\text{int}} = 0.0555$)
Final R indices [$I > 2\sigma(I)$]	$R_1 = 0.0277$, $wR_2 = 0.0711$	$R_1 = 0.0383$, $wR_2 = 0.0905$
Final R indices (all data)	$R_1 = 0.0347$, $wR_2 = 0.0736$	$R_1 = 0.0775$, $wR_2 = 0.1127$
Largest difference peak and hole (e \AA^{-3})	0.354 and -0.614	0.389 and -0.490

Information concerning crystallographic data collection and structure refinement details are summarised in Table 1. Selected bond lengths and angles for the two structures are given in Tables 2 and 3. Hydrogen-bonding geometry for the two structures is described in Tables 4 and 5.

Table 2
Bond lengths (in Å) and angles (in °) for [Co(picOH)₂(H₂O)₂] (I)^a

Co(1)–O(1W)	2.0789(13)	O(1W)–Co(1)–O(1)	93.07(5)
Co(1)–O(1)	2.1105(12)	O(1W)–Co(1)–O(1) ⁱ	86.93(5)
Co(1)–N(1)	2.1245(15)	O(1W)–Co(1)–N(1)	89.15(6)
		O(1W)–Co(1)–N(1) ⁱ	90.85(6)
		O(1)–Co(1)–N(1)	78.23(5)
		O(1)–Co(1)–N(1) ⁱ	101.77(5)

^a Symmetry transformations used to generate equivalent atoms: (i) $-x, 2-y, -z$.

Table 3
Bond lengths (in Å) and angles (in °) for *mer*-[N(CH₃)₄][Co(picOH)₃]·H₂O (II)

Bond lengths			
Co(1)–O(1)	2.077(2)	Co(1)–N(1)	2.134(2)
Co(1)–O(4)	2.066(2)	Co(1)–N(2)	2.149(2)
Co(1)–O(7)	2.078(2)	Co(1)–N(3)	2.144(2)
Bond angles			
O(1)–Co(1)–O(7)	97.70(8)	O(4)–Co(1)–N(3)	98.16(9)
O(1)–Co(1)–N(1)	78.45(8)	O(7)–Co(1)–N(1)	87.93(8)
O(1)–Co(1)–N(2)	90.52(9)	O(7)–Co(1)–N(2)	171.45(9)
O(1)–Co(1)–N(3)	93.91(9)	O(7)–Co(1)–N(3)	78.93(8)
O(4)–Co(1)–O(1)	164.80(8)	N(1)–Co(1)–N(2)	96.08(9)
O(4)–Co(1)–O(7)	93.67(8)	N(1)–Co(1)–N(3)	163.84(9)
O(4)–Co(1)–N(1)	91.98(9)	N(3)–Co(1)–N(2)	98.22(9)
O(4)–Co(1)–N(2)	78.68(9)		

Table 4
Hydrogen-bonding geometry (distances in Å and angles in °) for [Co(picOH)₂(H₂O)₂] (I)^a

D–H···A	<i>d</i> (D···A)	∠(DHA)
O(1W)–H(1A)···O(2) ⁱ	1.799(19)	167(2)
O(1W)–H(1B)···O(1) ⁱⁱ	1.841(10)	168(2)
O(3)–H(3)···O(2)	1.83	146

^a Symmetry transformations used to generate equivalent atoms: (i) $x, 1.5 - y, 1/2 + z$; (ii) $-x, 1/2 + y, 1/2 - z$.

Table 5
Hydrogen-bonding geometry (distances in Å and angles in °) for *mer*-[N(CH₃)₄][Co(picOH)₃]·H₂O (II)^a

D–H···A	<i>d</i> (D···A)	∠(DHA)
O(3)–H(4A)···O(2)	2.577(3)	145.3
O(6)–H(6A)···O(5)	2.540(3)	147.2
O(9)–H(9)···O(8)	2.547(3)	145.5
O(1W)–H(1A)···O(1)	2.822(3)	172(3)
O(1W)–H(1B)···O(8) ⁱ	2.766(3)	169(4)

^a Symmetry transformations used to generate equivalent atoms: (i) $x, 1.5 - y, 1/2 + z$.

2.3. Instrumentation

FT-IR spectra were measured from KBr disks (Aldrich, 99%+, FT-IR grade) on a Matson 700 FTIR spectrometer. Elemental analyses for C, H and N were performed in the Microanalysis Laboratory of the University of Aveiro. Thermogravimetric analyses (TGA) were carried out using a Shimadzu TGA-50, with a heating rate of 10 °C/min. Magnetic measurements were performed using a Quantum Design SQUID (Superconducting Quantum Interference Device) magnetometer MPMS at the University of Lisbon (Portugal).

3. Results and discussion

3.1. Crystal structure of [Co(picOH)₂(H₂O)₂] (I)

The reaction under aqueous media between Co²⁺ and 3-hydroxypicolinic acid led to the formation of a highly crystalline, air- and light-stable product which was formulated as [Co(picOH)₂(H₂O)₂] (I) on the basis of single-crystal X-ray diffraction (Table 1) and elemental analysis. This structure shares striking similarities with those recently reported by Jin and co-workers [4], [Zn(picOH)₂(H₂O)₂] and [Mn(picOH)₂(H₂O)₂], also containing first-row transition metal cations.

Compound I is formed by neutral centrosymmetric [Co(picOH)₂(H₂O)₂] complexes (Fig. 1), in which the Co²⁺ centre is located at an inversion centre and six-coordinated to two N,O-chelating picOH[−] anionic ligands [bite angle of 78.23(5)°] plus two water molecules, {CoN₂O₄}, with the coordination geometry resembling a slightly distorted octahedron (Fig. 1 and Table 2). As found in the structures containing Zn²⁺ and Mn²⁺ [4], the water molecules are *trans*-coordinated (Fig. 1) with the O_{water}–Co–O_{water} vector not being exactly perpendicular to the {N₂O₂} plane of the octahedron formed by the two picOH[−] anionic ligands (Table 2). The vector is indeed tilted by a combination of ca.

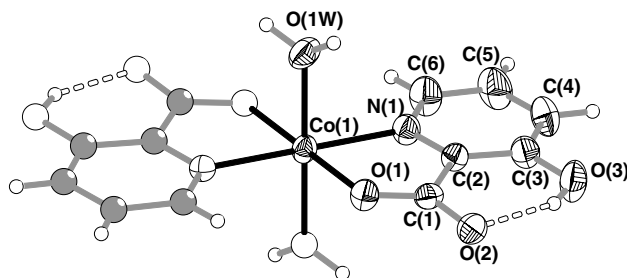


Fig. 1. Schematic representation of the neutral complex [Co(picOH)₂(H₂O)₂] of I, emphasising the slightly distorted octahedral coordination environment for the Co²⁺ metal centre. Non-hydrogen atoms belonging to the asymmetric unit are represented with thermal ellipsoids drawn at the 70% probability level. For selected bond lengths (in Å) and angles (in °) see Table 2. For details on the hydrogen-bonding geometry, see Table 4.

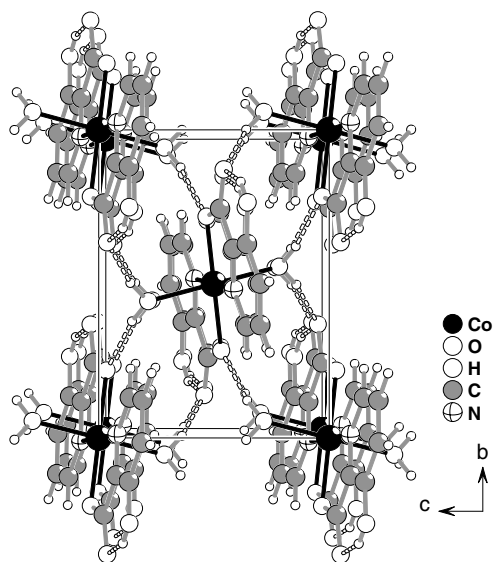


Fig. 2. Crystal packing of **I** viewed in perspective along the *a* direction, showing how the O–H···O hydrogen bond interactions (represented as dashed white-filled bonds) establish physical links between neighbouring [Co(picOH)₂(H₂O)₂] complexes. For details on the hydrogen-bonding geometry, see Table 4.

3.1° and 0.9° in both directions of the {N₂O₂} plane, values comparable with those registered for [Zn(picOH)₂(H₂O)₂] and [Mn(picOH)₂(H₂O)₂] (ca. 2.9/0.8 and 2.5/1.2, respectively) [4]. Interestingly, this distortion seems to be driven by the presence of extensive hydrogen-bonding networks in the crystal structures of these structures. In fact, apart from the homonuclear, intra-molecular and strong O–H···O hydrogen bond between the hydroxyl and the carboxylate groups (Fig. 1 and Table 4), each [Co(picOH)₂(H₂O)₂] moiety is further strongly hydrogen-bonded via the coordinated water molecules to another four neighbouring complexes, leading to a recurring R₂²(10) graph set motif [24] which expands the dimensionality of the structure into the two dimensions (see Fig. 2).

3.2. Crystal structure of *mer*-[N(CH₃)₄][Co(picOH)₃]·H₂O (**II**)

The substitution of the coordinated water molecules from the coordination sphere of **I** by a third 3-hydroxypicolinate ligand leads to the formation of an intriguing *mer*-isomer [Co(picOH)₃][−] complex anion (Fig. 3) which co-exists in the asymmetric unit of **II** with a tetramethylammonium cation plus a water molecule of crystallisation (not shown), corresponding to the empirical formula *mer*-N(CH₃)₄[Co(picOH)₃]·H₂O (**II**).

As in the previous structure, the crystallographically unique Co²⁺ centre appears six-coordinated, {CoN₃O₃} (Fig. 3), with a geometry resembling a distorted octahedron due to the geometrical constraints of the picOH[−] ligand: on the one hand, the chelating nature of 3-hydroxypicolinate leads to an average bite angle of

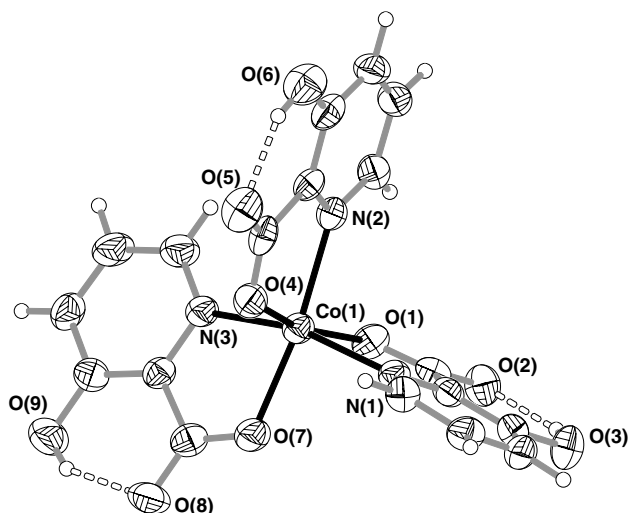


Fig. 3. Schematic representation of the anionic *mer*-[Co(picOH)₃][−] complex in **II**, showing the slightly distorted octahedral coordination environment for the Co²⁺ metal centre and the labelling scheme for selected atoms. Non-hydrogen atoms are represented with thermal ellipsoids drawn at the 70% probability level. For selected bond lengths (in Å) and angles (in °) see Table 3. For details on the hydrogen-bonding geometry, see Table 5.

ca. 78.7° which, although comparable with the analogous value for **I** [78.23(5)°], imposes some strain in the octahedral geometry; on the other, the presence of three large substituent ligands within the first coordination sphere leads to an inherent steric hindrance directly affecting the global geometry of the complex. In fact, these distortions are reflected in the ranges of the *cis* and *trans* angles of the octahedron which can be found within the 78.45(8)°–98.22(9)° and 163.84(9)°–171.45(9)° ranges, respectively (Table 3). The average Co–O and Co–N distances are almost identical (ca. 2.07 and 2.14 Å, respectively) and comparable with those found in related compounds [25,26].

The hydrogen-bonding network present in the crystal structure of **II** is not so extensive as that described for **I**. However, physical bridges via homonuclear and relatively strong O–H···O hydrogen bonds between neighbouring *mer*-[Co(picOH)₃][−] complex anions are assured by the water molecules of crystallisation (Table 5 and Fig. 4) which, along with interactions of the intra-molecular nature, lead to the formation of supramolecular hydrated {*mer*-[Co(picOH)₃]·H₂O}[−] anionic tapes running along the *a* direction (Fig. 4, perpendicular to the plane of the representation). This supramolecular arrangement is constructed from a recurring C₃²(7) graph set motif [24].

3.3. Magnetic measurements

Magnetisation (*M*) measurements were performed in the 2–270 K temperature (*T*) range and in a constant magnetic field of *H* = 100 Oe. No thermal irreversibility

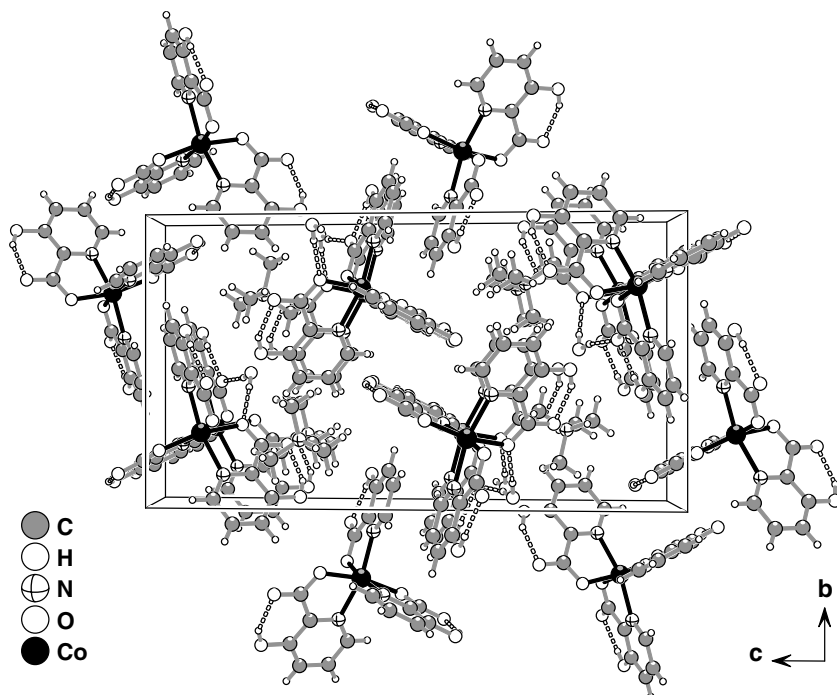


Fig. 4. Crystal packing of **II** viewed in perspective along the *a* direction, with the O–H···O hydrogen-bonding interactions represented as dashed white-filled bonds. The crystallisation water molecule establishes a physical link between neighbouring anionic *mer*-[Co(picOH)₃][−] complexes, leading to the formation of supramolecular hydrated {*mer*-[Co(picOH)₃]·H₂O}[−] anionic tapes running along the *a* direction. For details on the hydrogen-bonding geometry, see Table 5.

was observed since measurements taken with decreasing temperature gave identical results, either after cooling from ambient temperature to 2 K in zero applied magnetic field (zero field cooling), or after cooling under the measurement field.

Fig. 5 represents the magnetic susceptibility multiplied by the temperature (χT , with $\chi = M/H$) for compounds **I** and **II**. The temperature dependence indicates deviation from simple paramagnetic (Curie-like) ion behaviour. Such is ascribed to the influence

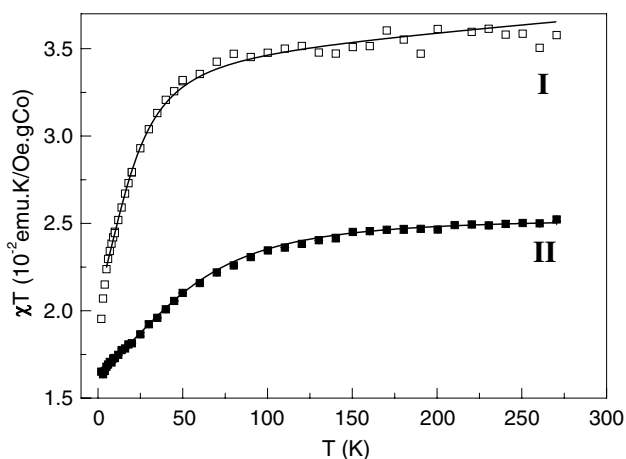


Fig. 5. Temperature dependence of the magnetic susceptibility multiplied by temperature (χT vs. T) for compounds **I** and **II**. Solid lines are fits to Eq. (1) (considering the influence of crystal field).

of crystal field of **I** and **II**, just like it is also observed in several mononuclear systems containing high-spin Co^{2+} ions in an octahedral coordination geometry [27]. The lowest energy levels of the Co^{2+} cations are Γ_6 and Γ_7 doublets, and in a first approximation one can consider that only these two are thermally populated. Hence the total susceptibility, can be described by [27]:

$$\chi = A \frac{g_z^2 \chi_z + 8g_x^2 \chi_x}{4T} + \chi_0, \quad \text{with}$$

$$\chi_z = \frac{1 + 9e^{-(2D/T)}}{1 + e^{-(2D/T)}} \quad \text{and} \quad \chi_x = \frac{1 + \frac{3T}{4D}(1 - e^{-(2D/T)})}{1 + e^{-(2D/T)}}, \quad (1)$$

where $A = N\mu_B^2/3k$, g_z and g_x are the Landé factors associated with *z* and *x* directions, respectively, D is the crystal field splitting and χ_0 is the residual temperature independent which accounts for diamagnetic contributions. Within this approximation, D includes the Γ_6 and Γ_7 energy gap and the influence of the orbital momentum [27]. Fitting the data to Eq. (1) (lines in Fig. 5) we obtain $D = 24$ and 65 cm^{-1} for samples **I** and **II**, respectively, in good agreement with the values expected for Co^{2+} cations (Ref. [27] and references therein). From the fitting, it is also feasible to calculate $g_x = 2.1$, $g_z = 2.3$ and $g_x = 1.8$, $g_z = 1.7$. Small variations of these parameters are not critical for the quality of the fit and are subject to absolute errors of the order of 0.1. Although at present we do not have a plausible

Table 6
Analytical and spectroscopic data for 3-hydroxypicolinic acid and compounds **I** and **II**

Compound	Elemental composition (%) ^a			Vibrational data (in cm ⁻¹) ^b			
	C	N	H	$\nu_{\text{asym}}(-\text{CO}_2^-)$	$\nu(\text{C-N})$	$\nu_{\text{sym}}(-\text{CO}_2^-)$	$\nu(\text{C-O})_h$
3 Hydroxypicolinic acid				1701s	1609s	1322s	1282s
I	38.05 (38.83)	7.38 (7.55)	3.55 (3.26)	1644s	1602s	1343s	1268s
II	46.31 (46.73)	9.93 (9.91)	4.83 (4.63)	1631s	1602s	1333s	1248s

^a Calculated values are in parentheses.

^b s: strong.

explanation for the difference between these values for the two compounds, the ratio g_z/g_x is ca. 1.1, in good agreement with the values reported for similar compounds (1.06) [27]. The differences registered for the crystal field splitting can be attributed to the influence of the donor atoms present in the Co²⁺ first coordination shell. In fact, compound **II** has one more pyridinic ring bound to the metal, which increases the crystal field splitting, in agreement with the spectrochemical series.

3.4. Vibrational spectroscopy

Selected and diagnostic FT-IR data for compounds **I** and **II** are given in Table 6 (only bands of 3-hydroxypicolinic acid sensitive to metal coordination are reported). Infrared spectroscopy confirms the coordination of picOH⁻ to the metal centres via the carboxylate group, with the asymmetric stretching $\nu_{\text{asym}}(-\text{CO}_2^-)$ mode showing shifts up to 70 cm⁻¹ to lower wavenumbers when compared with the values registered for the free ligand. Furthermore, the measured values of $\Delta[\nu_{\text{asym}}(-\text{CO}_2^-) - \nu_{\text{sym}}(-\text{CO}_2^-)]$ for **I** (301 cm⁻¹) and **II** (298 cm⁻¹) are clear evidence of the presence of carboxylate groups coordinated to the Co²⁺ centres in unidentate fashion [28], in agreement with the N,O-chelation described by the crystal structures (Figs. 1 and 3). The $\nu(\text{C-O})_h$ mode for **I** and **II** shows shifts up to ca. 14 and 34 cm⁻¹, respectively, possibly due to hydrogen-bonding involving the carboxylate groups and the water molecules (Tables 4 and 5). The typical stretching $\nu(\text{C-N})$ vibrational mode of substituted pyridines appears for the uncoordinated ligand at 1609 cm⁻¹ and shows small shifts (up to 7 cm⁻¹) for the two compounds (Table 6), in good agreement with N,O-chelation involving the nitrogen atom of picOH⁻.

3.5. Thermal analysis

Thermal decomposition of compound **I** occurs in a multi-step process between ambient temperature and ca. 500 °C leading to the formation of the stoichiometric amount of CoO (total weight loss of 78.1%, calculated 79.8%). The first weight loss (ca. 9.5%) occurs in the 80–180 °C temperature range (DTG peak at 150 °C) and is attributed to the release of the two coordinated

water molecules (calculated weight loss of 9.7%). Between 180 and 500 °C, a total weight loss of ca. 68.6% (DTG peaks at 353, 409, 418 and 432 °C) corresponds to the release of the organic component.

The thermal decomposition of **II** between ambient temperature and ca. 550 °C is slightly more complex than that of **I** with more overlapping decomposition steps corresponding to the oxidation of the organic molecules. However, as for **I**, at ca. 550 °C only the stoichiometric CoO residue remains with a total weight loss of ca. 88.6% (calculated 86.7%).

Acknowledgements

We are grateful to the Portuguese Foundation for Science and Technology (FCT) for their general financial POCTI programme supported by FEDER and the Ph.D. scholarships No. SFRH/BD/3024/2000 (to F.A.A.P) and SFRH/BD/10383/2002 (to N.J.O.S.). P.G. thanks CICECO for a research grant. We thank Professor Margarida Godinho for allowing us to perform the magnetic measurements at the Faculty of Sciences, University of Lisbon.

Appendix A. Supplementary data

Crystallographic data (excluding structure factors) for the structures reported in this paper have been deposited with the Cambridge Crystallographic Data Centre as supplementary publication no. CCDC-241918 and -241919. Copies of the data can be obtained free of charge on application to CCDC, 12 Union Road, Cambridge CB2 2EZ, U.K. (fax: (+44) 1223 336033; e-mail: deposit@ccdc.cam.ac.uk, and <http://www.ccdc.cam.ac.uk>).

Supplementary data associated with this article can be found, in the online version at doi:10.1016/j.poly.2005.01.002.

References

- [1] P.C.R. Soares-Santos, H.I.S. Nogueira, V. Felix, M.G.B. Drew, R.A.S. Ferreira, L.D. Carlos, T. Trindade, Chem. Mater. 15 (2003) 100.

- [2] E. Kiss, A. Benyei, T. Kiss, *Polyhedron* 22 (2003) 27.
- [3] S. Yano, M. Nakai, F. Sekiguchi, M. Obata, M. Kato, M. Shiro, I. Kinoshita, M. Mikuriya, H. Sakurai, C. Orvig, *Chem. Lett.* (2002) 916.
- [4] C.Y. Sun, X.J. Zheng, L.P. Jin, *J. Mol. Struct.* 646 (2003) 201.
- [5] S.M.O. Quintal, H.I.S. Nogueira, H.M. Carapuca, V. Felix, M.G.B. Drew, *J. Chem. Soc., Dalton Trans.* (2001) 3196.
- [6] S.M.O. Quintal, H.I.S. Nogueira, V. Felix, M.G.B. Drew, *New J. Chem.* 24 (2000) 511.
- [7] A. Dar, K. Moss, S.M. Cottrill, R.V. Parish, C.A. McAuliffe, R.G. Pritchard, B. Beagley, J. Sandbank, *J. Chem. Soc., Dalton Trans.* (1992) 1907.
- [8] S. Gatto, T.I.A. Gerber, G. Bandoli, J. Perils, J.G.H. du Preez, *Inorg. Chim. Acta* 269 (1998) 235.
- [9] A. Shaver, J.B. Ng, D.A. Hall, B.S. Lum, B.I. Posner, *Inorg. Chem.* 32 (1993) 3109.
- [10] R. March, W. Clegg, R.A. Coxall, L. Cucurull-Sanchez, L. Lezama, T. Rojo, P. Gonzalez-Duarte, *Inorg. Chim. Acta* 353 (2003) 129.
- [11] P.C.R. Soares-Santos, H.I.S. Nogueira, V. Felix, M.G.B. Drew, R.A.S. Ferreira, L.D. Carlos, T. Trindade, *Inorg. Chem. Commun.* 6 (2003) 1234.
- [12] P.C.R. Soares-Santos, H.I.S. Nogueira, J. Rocha, V. Felix, M.G.B. Drew, R.A.S. Ferreira, L.D. Carlos, T. Trindade, *Polyhedron* 22 (2003) 3529.
- [13] S.M.O. Quintal, H.I.S. Nogueira, V. Felix, M.G.B. Drew, *Polyhedron* 21 (2002) 2783.
- [14] T. Kottke, D. Stalke, *J. Appl. Crystallogr.* 26 (1993) 615.
- [15] R. Hoof, *COLLECT: Data Collection Software*, Nonius B.V., Delft, The Netherlands, 1998.
- [16] Z. Otwinowski, W. Minor, in: C.W. Carter Jr., R.M. Sweet (Eds.), *Methods in Enzymology*, vol. 276, Academic Press, New York, 1997, p. 307.
- [17] R.H. Blessing, *Acta Crystallogr., Sect. A* 51 (1995) 33.
- [18] R.H. Blessing, *J. Appl. Crystallogr.* 30 (1997) 421.
- [19] SMART. Bruker Molecular Analysis Research Tool v. 5.054[®] Bruker AXS, Madison, WI, USA, 1997–1998.
- [20] SAINTPlus. Data Reduction and Correction Program v. 6.01[®] Bruker AXS, Madison, WI, USA, 1997–98.
- [21] G.M. Sheldrick. SADABS v. 2.01, Bruker/Siemens Area Detector Absorption Correction Program Bruker AXS, Madison, WI, USA, 1998.
- [22] G.M. Sheldrick, *SHELXS-97*, Program for Crystal Structure Solution, University of Göttingen, 1997.
- [23] G.M. Sheldrick, *SHELXL-97*, Program for Crystal Structure Refinement, University of Göttingen, 1997.
- [24] J. Bernstein, R.E. Davis, L. Shimon, N.L. Chang, *Angew. Chem. Int. Ed.* 34 (1995) 1555.
- [25] K. Abe, K. Matsufuji, M. Ohba, H. Okawa, *Inorg. Chem.* 41 (2002) 4461.
- [26] Y.C. Liang, M.C. Hong, J.C. Liu, R. Cao, *Inorg. Chim. Acta* 328 (2002) 152.
- [27] O. Kahn, *Molecular Magnetism*, Wiley-VCH, New York, 1993.
- [28] G.B. Deacon, R.J. Phillips, *Coord. Chem. Rev.* 33 (1980) 227.